An Elsevier Indexed Journal ISSN-2230-7346

Journal of Global Trends in Pharmaceutical Sciences

FORMULATION DEVELOPMENT AND *IN VITRO* & *IN VIVO* CORRELATION OF MUCOADHESIVE NANOSPHERES OF ISONIAZID

Vishnu Vardhan Reddy Beeram[1], Krupanidhi S1, Venkata Nadh[2], B. Syed Salman[3]

[1]Department of Biotechnology, Vignan's University. Vadlamudi, Guntur – 522213, India
[2]GITAM University, Bengaluru Campus, Karnataka – 561203, India,
[3]Department of Pharmaceutics, Mahathi College of Pharmacy, Madanapalle, Andhra Pradesh, India.

***Corresponding author E-mail:** srivyshu.pharma@gmail.com

ARTICLE INFO

Key Words

Isoniazid, PLGA, Nanospheres, Tuberculosis

Access this article online
Website: https://www.jgtps.com/
Quick Response Code:

ABSTRACT

Isoniazid is a first line antitubercular agent, upon repeated dosing produces hepatotoxicity by oral administration. Pulmonary drug delivery can avoid the toxicity of drugs intended for tuberculosis. The study is an attempt to prepare mucoadhesive inhaled nanospheres of Isoniazid with polylactic glycolic acid (PLGA). The optimized formulation was selected using Box Behnken design. The lead formulation (F4) freeze dried INH-PLGA nanospheres (INH-NP's) was selected and prepared by high speed homogenization technique. INH-NP's characterization done by particle size, poly dispersity index, zetapotential, scanning electron microscopy (SEM), Fourier transform infra red spectroscopy (FTIR), Differential scanning colorimeter (DSC), stability studies, entrapment efficiency, *ex vivo* sheep nasal mucoadhesion studies,*In vitro* diffusion and drug release, cytotoxicity studies and *In vivo* pharmacokinetic studies using both serum and tissue analysis. Finally the nanospheres tested for their effect on mycobacterium using *in vitro* and *in vivo* microbial studies. The optimized INH-PLGA nanospheres showed 56.8 ± 2.22nm, 0.931± 0.02, -1.6±1.22mV, 94.42±2.20% and 96.80±2.60% of mean particle size, poly dispersity index, zeta potential, entrapment efficiency and drug content respectively. Potential interactions of INH and PLGA were found in FTIR and DSC studies without interfere in INH drug release. Bioadhesive property of INH-PLGA nanospheres was also found be enhance to 82±0.98%and permeation 89.54±1.20% compared to pure INH.The cytotoxicity studies resulted against the A549 showed significant IC50 ranges from 9.8 to 10.7. The bio distribution studies by IV and inhalation resulted that the Inhalation of INH-PLGA nanospheres with sustained drug release in the lungs. Mycobacterium studies revealed that the INH-PLGA nanospheres showed significant Log10CFUs in*in vitro* and in *in vivo* (18 days and 6 weeks) in mice compared to pure INH. The overall study concluded that the INH-PLGA nanospheres are potential pharmaceutical and therapeutic outcome for tuberculosis.

INTRODUCTION

Tuberculosis (TB) is one of the common life threatening diseases affecting the lung and Pulmonary system in all the age groups (1). According to the study conducted during 2016, more than 10.4 million new cases are observed and they remain stable with TB, in 2017 it was increased upto 11.1 million cases among 5.8

million men, 3.2 million women and 1.0 million children. Among deaths of 1.3 million people HIV negative, 300 000 deaths are HIV positive(2). The problem with TB therapy is drug resistance. In 2017 it is estimated that 558 000 people were developed rifampicin resistance and 82% had multi drug resistance. Worldwide, India (24%), China (13%) and the Russian Federation (10%) are top 3 countries recommended 6 months regimen of first line anti TB drugs are isoniazid, rifampicin, ethambutol and pyrazinamide (3). Resistance to drug and adverse events due to untoward reactions are the common associated problem with the use of anti-tubercular drugs. INH is considered as the first line drug for treating pulmonary tubercular infections caused by tubercle bacilli (4). INH as a drug of choice for the tuberculosis acts by interfering in the enzyme connected metabolic pathway of tubercular microorganisms. This nicotinic acid derivative shows its anti-bacterial activity by directly attacking and inhibiting the cell wall lipid and nucleic acid synthesis of tubercular species (5). INH is highly active against *Mycobacterium tuberculosis* with 0.01 to 0.25 µg/ml of MIC value, acts only for growing tubercle bacilli but not for nongrowing bacilli (6). The INH resistance was found to be more frequent to drug resistant clinical isolates with 20-30% incidence range(7). Hence, need to develop or control over the resistance of INH and other first line anti TB drugs and its combinations(8). INH is widely administered oral medication from mid-19th century to till date in the form of tablet with a daily dose ranging from 50-300mg. Isoniazid is metabolized in the liver through acetylation by N-acetyltransferase, which produces acetylisoniazid and isonicotinic acid. It is excreted by kidney as inactive metabolite (70-96%) and sometimes through urine as free Isoniazid (7%) and conjugated form (37%) depends on acetylation (9). The undesirable side effects are relatively high with the use of solid dosed INH tablet due to its elevated distribution in urinary system and liver such as peripheral neuropathy and hepatits (10). Considering this as a major limitation researchers are focusing on novel and alternate approach to enhance the activity of such potent and lifesaving medication in the form of nasal dosage forms like metered dose and dry powder inhalers (11). To overcome the all the difficulties with oral Isoniazid administration, many researchers prepared proliposome Powders for inhalation (12) and chitosan microspheres (13). The existed formulations are reported to produce better pharmaceutical approaches among the existed formulations. Nanospheres mediated dry powder Inhalation was thought as a novel approach for inhibiting the growth of active tubercle bacilli in the infected respiratory site due to its thermal stability, drug carrying capability, ease of drug incorporation within the matrix system and rate controlled delivery of drug (11). The delivery system can show better performance by increasing the drug concentration at the respiratory site of lungs and thereby avoiding the systemic toxic impact (14). In specific, freeze dried biodegradable polymeric nanospheres of INH using PLGA was prepared and targeted to the pulmonary system by utilizing powder inhalation technique (15). Evidence shows that PLGA as polymeric carrier is found successful in nasal delivery of Diazepam (16), olanzapine nanoparticulates (17), Tetanus toxoid (18), Lorazepam (19), α-cobrotoxin microparticulates (20), mucoadhesive peptide (21) and encapsulated vaccine microspheres (22). Henceforth, a research attempt is made to envisage formulation of INH nanospheric powder inhaler for nasal delivery to treat tubercular infections. The prepared Isoniazid-PLGA nanospheres (INH-NP's) were characterized for various physicochemical properties for confirming its geometrical size, shape and drug content. On further continuation *in vitro* studies was executed for drug release from INH-NP's using dialysis membrane as a barrier in Franz diffusion cell (FDC) (23). The pharmacokinetic studies of nanospheres were performed in male albino Wistar rats for drug distribution and concentration in various organs like lungs, kidneys and liver. An optimized INH-NP's was thought to increase the concentration of drug in pulmonary site that in turn inhibit the mycobacterial activity and its growth.

MATERIALS

A gift sample of INH (Yarrow Chemicals, Mumbai) was used as anti-tubercualar agent for nanospheric formulation.

PLGA was used as a lipid material for loading INH. Poly vinyl alcohol commonly known as PVA was selected as a surfactant. Methanol, ethanol and acetone (Merck specialties Pvt. Ltd.) were used as Organic solvents. All the buffering agents and water for HPLC for the study was supplied by RL fine chemicals, India.

METHODS

Solubility profiling of INH in different solvents: In order to find out the most suitable solvents for further studies solubility profiling plays an important role. An excess amount of INH was added to 10ml of different solvent system (Ethanol, water and simulated salivary fluid) taken in a series of stopper conical flask. The resultant solvent mixture was kept for shaking on a rotary shaker for 24hr at room temperature (24). The equilibrated samples were strained using whatmann filter paper having a pore size of 0.45µm and the filtered drug solution were diluted suitably in their respective solvent and subjected to UV-Spectroscopic analysis at 263nm (25). The solubility trial was conducted in triplicate to minimize the errors in the results obtained.

Preparation of PLGA nanospheres of INH by high pressure homogenization technique: Anti-tubercular nanospheres were prepared by matrixing INH in a biodegradable PLGA polymer by mechanism of high pressure homogenization in presence of an emulsifying agent (26). In brief, an organic phase containing 1:3 ratios of INH in ethanol solvent was prepared and mixed with different concentration of PLGA (5, 10 and 15%w/w). The ethanolic component of INH-PLGA is emulsified using variable concentrations of PVA under constant stirring. The process involves slow drop wise addition of dispersed phase (INH-PLGA) to continuous phase (PVA) (27). Thus formed emulsified mixture is introduced into high pressure homogenizer (HPH) for further process to obtain particle of desired submicron range. The principle involves pressurized movement (~100-2000 bars) of INH-PLGA emulsion fluid through the narrow miniature for a short distance at a high velocity (~600miles/h) between the piston valve and seat of HPH (28, 29). The suspended nanospheres were cold processed (3°C) in an ultracentrifuge at 30,000rpm for 15min, continuously washed thrice with double deionized water and freeze-dried for 38h.

Optimization by Box Behnken design: As a part of optimization technique, Box Behnken design (3^3) was incorporated for investigating the factors involved in formulating the INH-NP's. The individual independent variables like % w/w concentration of both polymer (X_1) and surfactant (X_2) along with homogenization time measured in minutes (X_3) were fitted to Design-Expert software (version 9 trial stat-Ease Inc., Minneapolis, USA). Based on individual variables the experimental optimization was subjected to coding at 3-different levels as low (-1), medium (0), high (+1). Subsequently the dependent variables such as particle size in nanometer range (Y_1) and % Zeta potential (Y_2) were measured (20). A sum total of 17 runs were generated by this design with 3 center points and 12 factorial points as shown in Table 2. The polynomial equation produced by Box-Behnken design was followed as.

$$Y= a_0+a_1x_1+a_2x_2+a_3x_3+a_{12}x_1x_2+a_{13}x_1x_3+a_{23}x_2x_3+a_{11}x_1^2+a_{22}x_2^2+a_{33}x_3^2$$

Independent and dependent variables and their separate levels shown in the Table 1

Freeze drying process: Freeze drying is a technique of conserving the physical and chemical stability of nanospheres by removing the water molecules. During freeze drying the nanospheres were vitrified by matrixing with a cryoprotectant (CPA) namely mannitol. The PLGA nanospheres were transferred to glass vials having different concentration of mannitol (5, 12.5 & 15%) aqueous solution in an equal ratio of 1:1 and mixed thoroughly. The contents of glass vials were supercooled in a liquid nitrogen environment at a temperature of -20 °Cto -80°C for 23 hours. Thus formed frozen spheres were lyophilized (ScanVac lyophilizer) at a vacuum pressure of ~4.35 psi for 23 hours. The freeze dried samples were rehydrated by reconstituting with simulated salivary fluid (SSF) for particle characterization, *in vitro* and *in vivo* studies (30,31)

Measurement of particle size, poly dispersity index (PI) and zeta potential of nanospheres: The physicochemical characterization of nanospheres is carried out in a Zetasizer (Malvern- ZEN 3690) fitted with a laser beam of Helium – Neon (He-Ne). The technique is based on dynamic light scattering (DLS) that has the ability to render information about mean particle size and charge mobility under the applied potential difference. About 100µL of freeze dried INH nanospheres (INH-NP's) is incorporated in 1ml of de-ionized water filled in a disposable zeta cell. The aqueous mixture of particulate system was placed in a He-Ne pathway at a definite angle of 90^{o} for investigating particles size. The means values of the particle diameter and its width is traced to obtain PI as a measure of its particle size distribution. On further continuation, laser doppler electrophoresis (LDE) was performed with the zetasizer to obtain zeta potential value. In specific, zeta potential is calculated by fitting data in Henry's equation obtained by interaction between the mobility of charge and the applied voltage (32,33).

Scanning electron microscopy (SEM)

The dried microscopic aggregates of PLGA nanospheres were studied for morphological characters using SEM. The particles of interest were made conductive with metallic gold (100 A°) by coating under the noble gaseous atmosphere of Argon. The micrographs obtained were observed for particle regularity and its dimensions (34,35).

Fourier transforms infrared spectroscopy (FTIR): This study involves closely examining the Infrared spectral peaks of pure drug (INH) and its physical mixture containing PLGA. The samples were prepared by milling with KBr powder (particle size <5mm) and compressing it into pellets using Quick handi-press. Thus prepared sample-KBr pellets were placed inside the sample holder of IR spectrometer followed by testing the absorption intensity in the mid wavelength range of 4000-400 cm^{-1}. Thus obtained graphical data were interpreted for identifying the functional groups and compatibility of drug and its excipients (36).

Differential scanning colorimetry (DSC): The drug, excipients, its physical mixtures and optimized INH-NP formulation were subjected to thermal analysis in a differential scanning colorimetry (make and model) run at a predetermined temperature range (50-500^{0}C). The samples of known mass to be analyzed was dropped into aluminium crucible and placed inside the differential scanning colorimeter. The crucible was heated in presence of inert atmosphere of Argon gas at a rate of 10^{0}C.min^{-1} and observed for the elution of peak. Thus obtained peaks were subjected to analysis of enthalpy of melting (J/g), Peak temperature (^{o}c) and crystallinity index (37).

***Ex vivo* mucoadhesion studies:**

In-vitro mucoadhesive studies were performed as per the standardized procedure mentioned earlier (38). The mucoadhesiveness of nanospheres was carried out using the fresh nasal mucosa membrane of sheep obtained from the local slaughter house. We ideally preferred to use the septum part of nasal mucosa segregated from the superior conche (39). The sustainability and bioadhesiveness of INH loaded nanospheres in nasal mucosa was tested in phosphate buffer (pH 6.8). Prior to mucosal adhesion test, the weighed samples of INH-NP's (W_o) were wetted by immersing in phosphate buffer pH 6.8 for 5min maintained at 37±0.5°C. The local adhesion test of INH-loaded nanospheres in the lungs was outlined by just making the nasal mucosa contact with surface of pre-weighed nanospheres contained in a 50ml beaker. The unadhered INH-NP's were oven dried at a temperature of 60°C till a constant weight is obtained (W_r). The mucoadhesion property of drug in nanospheres was calculated by percent adhesion (% AN) test Equation 1.

$$AN(\%) = \frac{W_o - W_r}{W_o} \times 100 \qquad (1)$$

***In vitro* diffusion studies:** *In vitro* drug release studies of INH-NP's were performed using Franz diffusion cell having an effective diffusional area of 1.5 cm^{2}. The diffusion cell is comprised of two portals namely donor and acceptor compartment surrounded by a water circulating jacket for maintaining temperature of 37 ± 0.5^{o}C (40). The acceptor port was filled

with 30ml of SSF having pH 6.8 to mimic the human salivary fluid. As a diffusion barrier, dialysis membrane with a molecular weight of 12000-13000 Da (Himedia) and an average pore size of 0.45µm was used. The dialysis membrane (2×2 cm^2) was sandwiched between the donor and receptor compartment after activating the pores for 12 hours in SSF. Finally the donor chamber was filled with unit dose (10 mg/ 5mL) of INH-NP's dispersion and the permeation study was run for a time period of 23h in triplicate. The permeation study was carried out at an invariable rotation speed of 50rpm and 5ml receptor fluid was withdrawn from the sampling port at varied time points (0, 2, 3, 6, 8, 10, 12, 13, 16, 18, 20, 22, 23 hrs). The sink condition was well maintained throughout the diffusion studies by replacing equal volume of SSF in receptacle after collecting receptor phase at every time point. The amount of INH permeated across the dialysis membrane was estimated by UV-Spectroscopy at 263nm after suitably diluting the receptor fluid samples obtained at different time period against blank (SSF).

Entrapment efficiency: The optimized formulations of all INH-NP's entrapped and absorbed inside the PLGA core were systematically assessed for entrapment efficiency. About 5ml (equivalent to 10 mg of drug) of nanospheres dispersion was incorporated into Eppendorf tubes. The microcentrifuge tubes were placed inside the loop of ultracooling centrifuge and the same were centrifuged at 1500rpm for 30mins at 3˚C. After centrifugation, the segregation of nanospheres from the dispersion were facilitated by passing it across 0.35µm membrane filter. The supernatant liquid after successive dilution was subjected to UV spectrometric analysis against the blank at a wavelength of 263nm to determine the amount of encapsulated drug. The % encapsulation efficiency (%EE) was calculated using the equation 2.

$$\%EE = \frac{Amount of drug added - Amount of drug in aqueous phase}{Mass of drug added} \times 100 \quad (2)$$

Drug content (assay) determination: The INH content encapsulated in the PLGA nanospheres was determined by adding 1ml (2mg INH) solid dispersion of optimized formulations into a 10ml volumetric flask. The dispersion was diluted and total volume was made up to 10ml using methanol. Finally, the alcoholic mixture was filled into centrifuge tube and subjected to ultracentrifugation for a stipulated time of 15min maintained at a centrifugal speed of 10,000rpm. Thus obtained supernatant liquid was carefully aspirated and filtered using cellulose impregnated Whatman filter paper having a pore size of 0.45µm. The clear liquid was diluted suitably with methanol and the absorbance measured at a spectroscopic wavelength of 263nm for real drug content. The amount of drug content present inside the PLGA shell is calculated by the Equation 3 (41).

$$\% Drug content = \frac{Amount of drug - Unentrapped drug}{Weight of INH nanospheres} \times 100 \quad (3)$$

Stability studies

The role of stability study was to explore the intactness of nanospheres under long term stability conditions (25˚C ± 2 ˚C / 60% ± 5% RH and 30˚C ± 2 ˚C / 75% ± 5%) for 6 months. The optimized formulations were packed and reserved well within the glass bottles with screw cap sealed. The samples were withdrawn from the stability chambers at initial, 03 and 06 months respectively as detailed in Q1A(R) of ICH guidelines for new substance and products. The parameters such as Z-average, PDI, Zeta potential, drug release pattern, drug content and entrapment efficiency were tested in triplicate (42).

***In vitro* drug release kinetics**

Several different kinetic models can be incorporated to interpret *in vitro* release kinetics of the drug from the optimized formulations. The most commonly reported experimental models are included in this particular research such as zero order, first order, Higuchi square root, Korsmeyer-Peppas and Hixson crowell cube root model. After obtaining the highest regression and correlation coefficient (R^2) of the formulations, the best fit model was decided. The INH-NP's release rate

and its mechanism of release were analyzed by fitting the data in the following equations.

$$Q = K_0 t \quad (4)$$
$$LogQ = K_1 t \quad (5)$$
$$Q = K_2 t^{1/2} \quad (6)$$
$$Mt/M\infty = Ktn \quad (7)$$
$$\sqrt[3]{Q_0} - \sqrt[3]{Q_t} = \mathrm{K_{HC}t} \quad (8)$$

The total amount of drug release *(Q)* in both initial and at time *t* is expressed as *Q*. Likewise, the release rate constant at zero and first order kinetics is symbolized as K_0 *and* K_1 respectively. While considering Higuchi model the drug diffusion is expressed as K_2 at time $t^{1/2}$. In Korsmeyer-Peppas equational design a fraction of drug release is expressed in terms of $Mt/M\infty$ in time t, K is a constant associated with the structural and geometric characteristic of the difffusional device, *"n"* relates to exponential indication of mechanism of drug diffusion. The *"n"* value differs relating to Fickian (< 0.5) and non-Fickian (0.5-1.0) diffusion. K_{HC} is the rate constant obtained according to the Hixon and Crowell equation ($\%h^{-1}$) at time *t*(43,44).

***In-Vivo* evaluation of INH-NP's**

Pharmacokinetic studies

Healthy, naïve, albino Wistar rats (n=6, Male : Female 1:1) weighing 180 – 200 g used for bioavailability studies and were fasted for 12h prior to the experiment but had free access to water. INH-NP's were administered by oral feeding tube at the dose of 2.3mg/m2 of INH under mild anaethesia, blood samples were collected via the caudal vein at 0, 0.25, 0.50, 0.75, 1, 1.25, 2, 3, 6, 8 and 12 hours (in tubes with anti coagulant) and centrifuged immediately and the plasma obtained was stored at -200ºC until further analysis.

Quantification of plasma concentration: INH plasma concentration was determined by HPLC of C18-column (Analytical technologies 2000, India) analysis using Analytical technologies software at desired nm. A 200µl plasma sample was placed into a centrifuge tube and 200µl of methanol was added and shaken vigorously for 30s at room temperature. After centrifugation at 3000 rpm for 15 min, the supernatant was separated and analyzed. Calibration curves were prepared by linear regression analysis of the plot of the peak area against concentration of INH. The concentration of INH in plasma samples was determined from the area of chromatographic peak using the calibration curve.

Data analysis: Total calculations were done by software winnonlin noncompartmental analysis program 6.3.0.39 core version 03 jun2007 Peak concentration (Cmax) and time of peak concentration (t_{max}) were obtained directly from the individual plasma-concentration time profiles. Half life ($t_{1/2}$) was calculated from the terminal slope of the plasma concentration-time curves after logarithmic transformation of the plasma concentration values and application of linear regression. The basic calculations are based on the area under the plasma concentration versus times curve (zero moment) and the first moment curve (AUMC). The AUC can be calculated as before using the trapezoidal rule. The first moment is calculated as concentration times time (Cp x t). The AUMC is the area under the (Cp x t) versus time curve. Both the $AUC_{0\rightarrow t}$ and $AUMC_{0\rightarrow t}$ were calculated using the trapezoidal method. The area under the curve (AUC) determines the bioavailability of the drug for the given same dose in the formulation.

Bio-distribution studies of Drug loaded INH-NP's: For *in vivo* pharmacokinetic studies, healthy, naïve, male albino wistar rats (n=6) weighing 160–180 gm were used. The protocol was duly approved by the Institutional Animal Ethics Committee (IAEC) .

Route of administration: Inhalation: Pre-trained test animals were administered single dose of 100 mg of nanospheres by inhalational route, the required dose of drug loaded nanospheres were nebulized for 30 sec using an in house apparatus to obtain inhaled dose of 100mg/animal. Before dosing the rats were trained for 30 days to accept restraint & application of an infant inhalation mask attached to our in-house apparatus.

Sample collection:

Collection of blood and tissue samples: Blood samples were collected prior to inhalation, ten minutes after inhalation and

subsequently 1, 2, 3, 8, 12 and 23 after inhalation in mildly anaesthetized animals by tail incision. After blood collection, tissues of interest namely lungs, liver and kidney were excised under deep anaesthesia using ketamine-Xylazine by opening thoracic cavity and preserved in triple distilled water at -20-20ºC. The collected organs are sliced and homogenized at 6000 rpm for 20 min. The tissue fluids are collected and centrifuged at 3000 rpm for 10 min and finally the supernatant is collected and analyzed by HPLC.

Collection of broncho-alveolar lavage: Test animals were sacrificed**,** theirthoracic cavity is opened; lungs intact with trachea are excised. The trachea was cannulated & lungs were repeatedly lavaged with chilled PBS (containing 0.5 M EDTA), broncho alveolar fluids were pooled, centrifuged and macrophages obtained were counted and kept at -20ºC for further analysis.

Sample preparation for analysis: To 150 ml aliquots of plasma, 300 ml of de-protenizing agent (methanol) was added and the dispersion is vortexed for 2 min. The samples were centrifuged at 15,000 rpm for 10 min at 3ºC and supernatant is collected. INH was extracted using 3 ml portions of chloroform-butanol (70:30 %v/v) and vortexed for 1min followed by centrifuging at 3000 rpm for 10min. supernatant was decanted , process was repeated for 3 times & supernatants was pooled. The collected supernatants were diluted and analyzed by HPLC.

Tissue sample preparation

A 20%w/v aqueous tissue homogenates were prepared in cold 50M KCl. The homogenates were centrifuged at 15,000rpm for 10min at 3ºC and the clear supernatant thus obtained was used further. To 150µL aliquot of the clear tissue homogenates, 300µL of the methanol was added and the dispersion was vortexed for 2min. The samples were then centrifuged at 15,000rpm for 10min at 3ºC. The supernatant was collected and an equal volume of water was added. The samples were then filtered (0.20µm nylon filters) and were injected into the HPLC system.

Bio-analytical HPLC method: The collected serum samples were analysed by HPLC (Analytical technologies Ltd) comprising C-18 column & UV detector. The mobile phase consist of Triethanolamine acetate : acetonitrile (97: 3 %v/v) at 263nm by iso-cratic elution method. The mobile phase was delivered at a flow rate of 0.9 ml/min and The injection volume was 20µL and the analysis was performed at 30ºC.A wash program which increased the % methanol was included at the end of drug elution to ensure washout of all interfering excipients. Spectral purity analysis of the drugs peak over a range of 200–300 nm was performed. The accuracy and precision of the developed method for determination of drug was comparable to the isocratic methods described in USP.

Data Analysis: The pharmacokinetic parameters were calculated based on a non-compartmental body model. The area under the concentration–time curve from time zero to time (AUC0–t) was calculated using the trapezoidal method. Peak concentration (Cmax) and time of peak concentration (Tmax) were obtained directly from the individual plasma concentration–time profiles. The area under the total plasma concentration–time curve from time zero to infinity was calculated using Equation 9.

$$AUC0-\infty = AUC0-t + Ct/Ke \qquad (9)$$

where Ct is the concentration observed at last time and Ke is the apparent elimination rate constant obtained from the terminal slope of the individual plasma concentration. Time courses of serum drug concentration following inhalational route were analysed by winNonLin software program version 5.1 (pharsight corp NC).

Statistical analysis: All experiments were repeated at least three times. Results are expressed as means ± standard deviation. A difference between means was considered significant if the "p" value was less than or equal to 0.05.

RESULTS AND DISCUSSION

Solubility profiling in three different solvents: The experimental results of INH solubility in ethanol, water and simulated saliva fluid (SSF) was found to be 25.29±0.3448, 0.25±0.0305 and 6.24±0.0153 respectively. It is clear observation that each solvent has diverse impact on solubility of the drug. INH was showing progressive solubility in ethanol and water, but the solubility was comparatively less in SSF. The formulated INH nanospheres has to pass through the salivary secretion of oral mucosa henceforth SSF was considered as diffusion and release media for further studies. Because the SSF was reported to showed better release pattern in mucoadhesive buccal film bearing progesterone (45) and Gelatin Nanofiber Scaffolds (46).

Preparation and characterization of INH-NP's: As approved by FDA, polylactic-co-glycolic-acid (PLGA) is biodegradable and biocompatible in nature that gives promising results was used as a drug targeting polymer (47). In order to achieve targeting of drug to specific cells and to portray its biological activity, selection of polymers and the method of preparation are the most important components. Initially the drug was solubilized in ethanol and incorporated inside the PLGA in presence of PVA under the influence of high pressure homogenizer to obtain particles of nano-size. The encapsulation of drug inside the polymeric matrix of PLGA plays a vital role to showcase the targeted mechanism of action in pulmonary tuberculosis (48). In the present investigation an attempt is made to extract the anti-tubercular benefits of INH bound inside the hydrophobic capsule shell of PLGA polymer. In order to corroborate the size, shape, structure and morphology of the prepared nanospheres various physicochemical tests were performed that are portrayed in respective tables and figures.

Determination of nanospheres size: In order to achieve the particle size of nanometer range, concentration of PLGA (polymer) and PVA (surfactant) along with the homogenization time (mins) were considered as deciding factors. As per the Box-Behnken design, a total of 17 runs were experimented with combination of different variables to achieve particles of nanometer range and desired spherical characteristics. In this aspect a 5%w/w PLGA level was experimented in presence of varied PVA and homogenization time, the particle size was found to range between 56.8±2.22 to 148.1±3.42nm. Furthermore at the PLGA concentration of 10 and 15%, the particle size was found to increase in the range of 154.5±2.44 to 226.2±3.02nm and 269.5±3.60 to 369.5±2.62nm respectively. The overall values obtained clearly specify that the particle size was found to increase with the increase in PLGA concentration. The results of the study was supported by the previous studies i.e PLGA produced smaller particle size with uniform distribution of benzydamine mucoahhesive buccal zel conducted by Gina SE., 2019 (49).Bhosale UV et al., 2011 reported PLGA is a better polymer for mucoadhesive formulation of acyclovir-loaded mucoadhesive PLGA nanoparticles by sustained drug release (50).Further the higher levels of surfactant concentration (3%) and homogenization time (15mins) was also found to lower the particle size.Pandey J et al., 2016 formulated successfully levocetirizine loaded Mucoadhesive Microspheres for Nasal Delivery with PLGA as a polymer with potentiality in maintaining the particle size (51). Of all the formulations prepared, F4 formulation stabilized using 5% PLGA and 3% PVA under homogenization for 10mins was found to give nanospheres of smaller particle range. When measured, the nanospheres of F4 was giving a mean diameter, PI and zeta potential of 56.8±2.22nm, 0.931±0.02 and -1.6±1.22mV respectively indicating unique physicochemical characters compared to other INH-NP formulations. The encapsulation efficiency and the drug content of all the INH-NP formulation obtained after subjecting to different centrifugal procedures were found fall in the range of 42.68±2.52 to 94.42±2.20% and 42.54±2.62 to 96.80±2.60% respectively. As explained earlier the Lead formulation (F4) having less particle size was found give optimal entrapment efficiency of 94.42±2.20% and drug content of 96.80±2.60%.

Table 1 Factors and its levels used as per Box Behnken Design

Variables	Factors X,Y	Levels used, Actual (Coded)		
		Low(-1)	Medium (0)	High (+1)
Independent variables				
Polymer - PLGA (%w/w)	X_1	5	10	15
Surfactant (%w/w)	X_2	1	2	3
Homogenization time (min)	X_3	5	10	15
Dependent variables		Constraints		
Particle size (nm)	Y_1	Minimize		
Zetapotential (%)	Y_2	Maximize		

Table 2 Optimized trial Run formulations for INH-PLGA nanospheres

Run	Polymer PLGA (%w/w)	Surfactant PVA (%w/w)	Homogenization time (min)
1	5	1	10
2	5	2	15
3	5	2	15
4	5	3	10
5	10	1	15
6	10	1	5
7	10	2	10
8	10	2	10
9	10	2	10
10	10	2	10
11	10	2	10
12	10	3	5
13	10	3	15
14	15	1	10
15	15	2	15
16	15	2	5
17	15	3	10

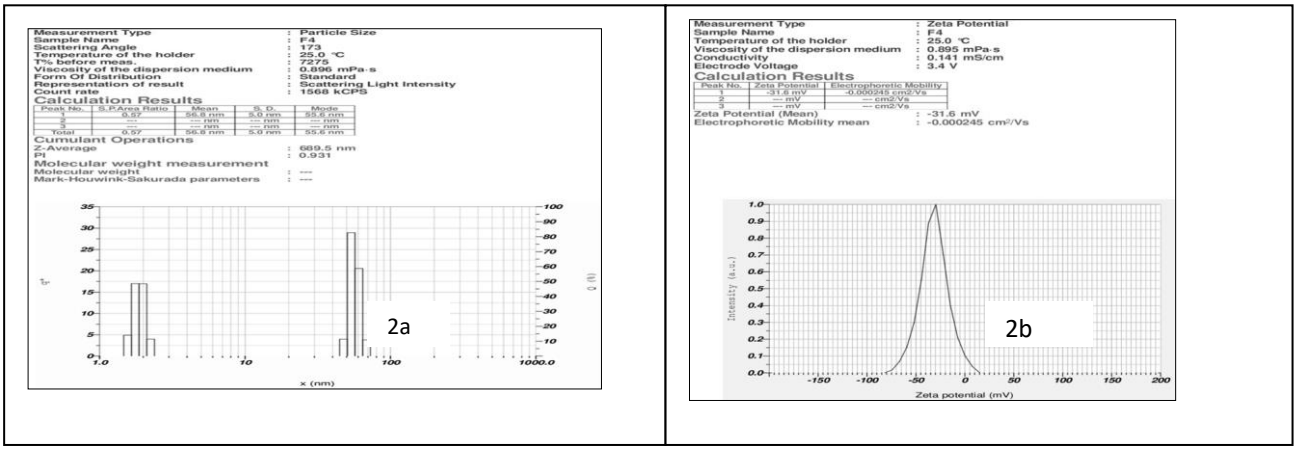

Fig.2 Particle size (a) and zeta potential (b) of F4 formulation observed under Zetasizer

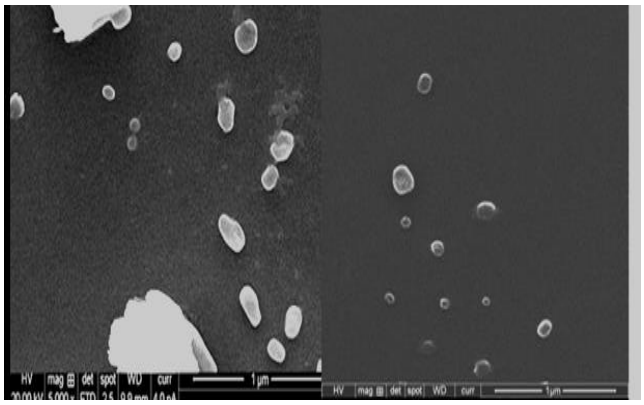

Fig.3. Scanning electron microscopic view of lead formulation (F4)

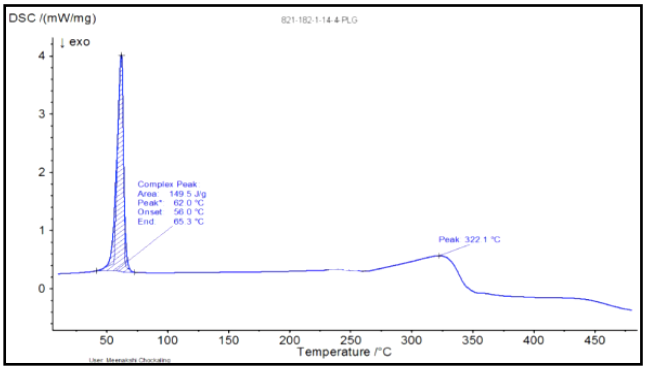

Fig. 3a DSC Thermogram of PLGA

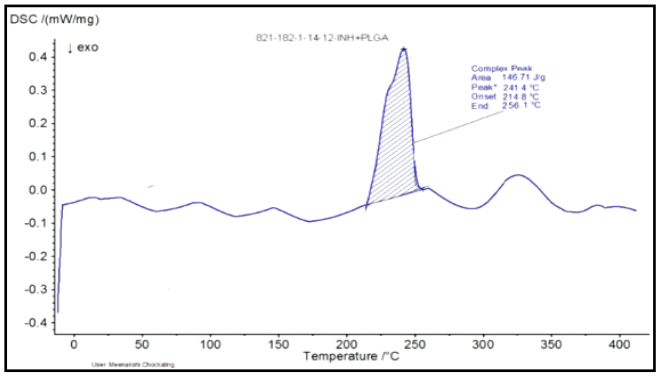

Fig. 3b DSC Thermogram of INH

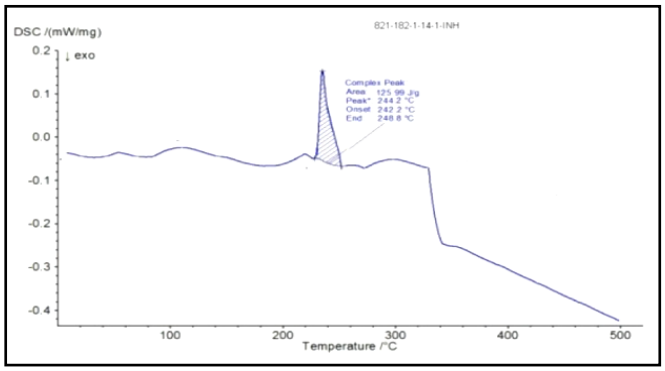

Fig. 3c DSC Thermogram of physical mixture of INH-PLGA

Table.3 Stability study data collected at different time points

Stability condition	Sampling interval (days)	Particle size (nm)	Zeta Potential (mV)	Poly dispersity Index (PI)	Entrapment efficiency (%)	Drug content %
25°±2°C/ 60±5% RH	0	56.8±2.22	-31.6±1.22	0.931±0.02	94.42±2.20	96.80±2.600
	15	56.8±2.12	-31.6±1.20	0.930±0.02	94.20±2.02	96.13±0.045
	45	56.8±2.22	- 31.6±1.20	0.930±0.02	94.12±2.12	96.04±0.084
	90	56.8±2.12	-31.6±1.22	0.930±0.02	94.12±2.14	96.03±0.025
40°±2°C/ 45±5% RH	0	56.8±2.22	-31.6±1.22	0.931±0.02	94.42±2.12	96.80±2.60
	15	56.8±2.12	-31.6±1.20	0.930±0.02	94.14±2.12	96.21±0.064
	45	56.8±2.22	-31.6±1.20	0.930±0.02	94.10±2.14	96.20±0.089
	90	56.8±2.22	-31.6±1.22	0.924±0.02	94.10±2.22	96.04±0.092

The data represents mean±SD (n=3)

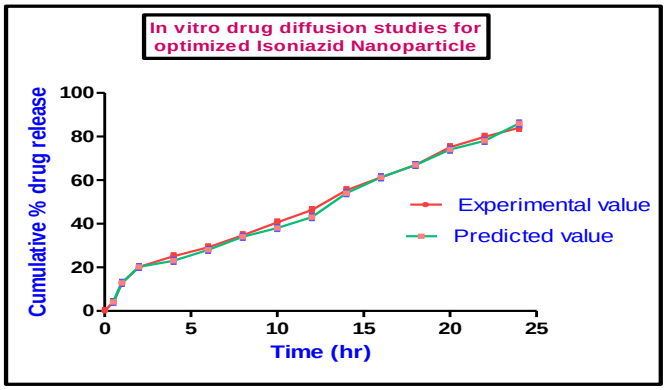

Figure 4: *In vitro* drug diffusion studies for optimized formulation F4

Table.4 Cytotoxic activity of INH-NP's

S.No	Concentration in (µM)	Cell lines and IC_{50} (µM)	
		INH	INH-NP's
01	0.1	8.2±0.08	10.2±0.51
02	0.2	8.9±0.07	9.8±0.37
03	0.4	9.1±0.26	9.4±0.31
04	0.6	8.8±0.58	10.7±0.15
05	0.8	8.8±0.17	10.2±0.74
06	1	9.2±0.43	9.9±0.83

Results are expressed as IC_{50} values in µM (n=3)

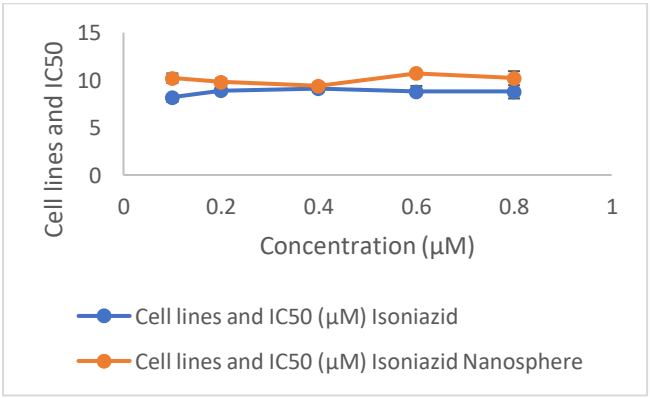

Fig. 5Cytotoxic activity of INH-NP's

Bio-distribution pharmacokinetics studies

Table 5 Bio distribution studies ofINH-NP's (F4) – IV Administration

Drug/route/origin	Tmax(hr)	Cmax(µg/ml)	AUC $_{0-\infty}$ (µg/ml/hr)	V_d (ml)	Clearance (ml/hr)
Lungs	2	19.16 ± 3.40	924 ± 44.42	256.84 ± 8.22	3.44 ± 0.40
Liver	3	26.24 ± 4.24	848 ± 42.38	202.2 ± 12.42	2.02 ± 0.22
Kidney	5	19.50 ± 2.22	540 ± 22.54	188.6 ± 10.4	2.44 ± 0.24

The data represents mean± SD (n=3)

Table 6 Bio distribution studies ofINH-NP's (F4) – Inhalation Administration

Drug/route/origin	Tmax(hr)	Cmax(µg/ml)	AUC $_{0-\infty}$ (µg/ml/hr)	V_d(ml)	Clearance (ml/hr)
Inhalation Lungs	22	38.42 ± 4.0	1824 ± 119.6	156.30 ± 4.64	1.0 ± 0.22
Liver	16	12.24 ± 0.90	326 ±10.80	454.32 ± 12.54	2.04 ± 0.40
Kidney	12	5.80 ± 0.12	208 ± 12.38	404.60 ± 8.50	2.24 ± 0.24

The data represents mean±SD (n=3)

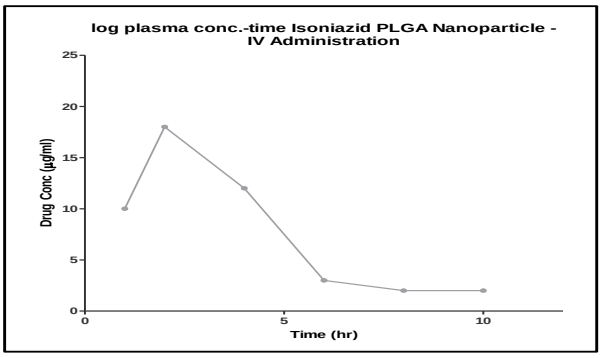

Fig6. XY plot for INH-NP's –IV administration

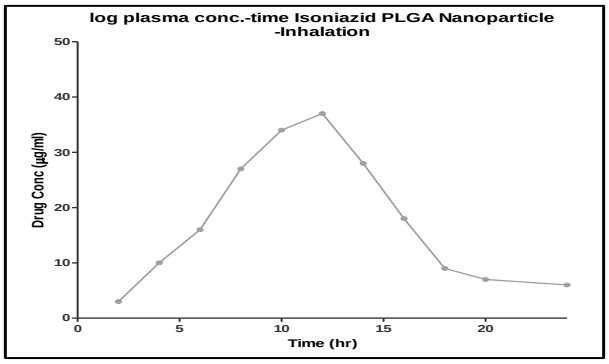

Fig 7. XY plot for INH-NP's –Inhalation administration

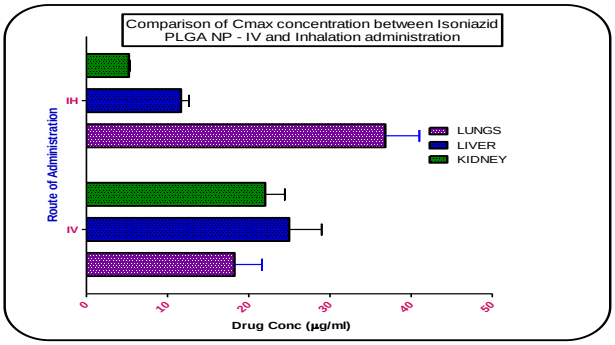

Fig. 8 Comparison of Cmax concentration between INH-NP's

IV and Inhalation administration

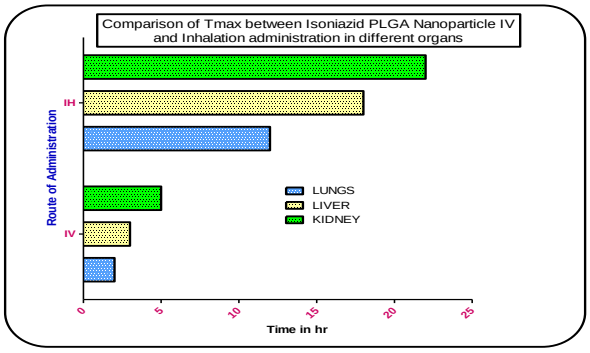

Fig. 9 Comparison of Tmax between INH-NP's IV and Inhalation administration in different organs

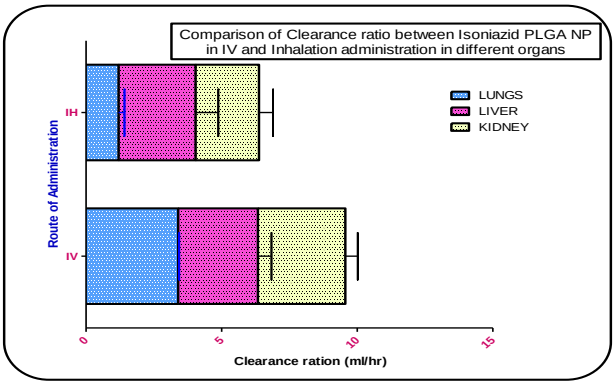

Fig. 10 Comparison of Clearance ratio between INH-NP's in IV and Inhalation administration in different organs

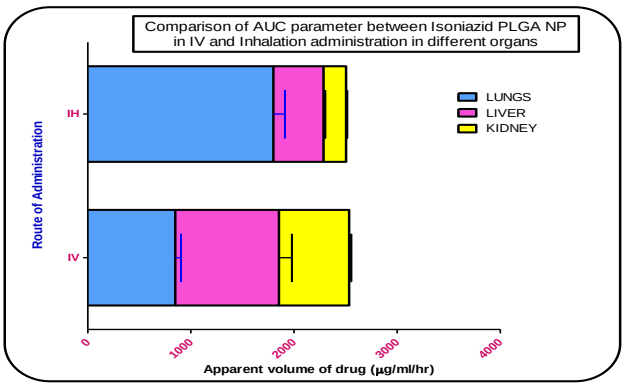

Fig. 11 Comparison of AUC parameter between INH-NP's in IV and Inhalation administration in different organs

Table 7 Growth of *M.tuberculosis* in culture medium and their control in different condition

Compound	Conc. µg/ml	Log_{10}CFU±SD (per ml)	% growth of microorganism compared with controls
Only culture	-	11.92 ± 0.24	100
Pure INH	25 mg/kg	8.44 ± 0.24	46.24
INH-NP's	Equivalent to 25 mg/kg	4.64 ± 0.24	44.14

The data represents mean±SD (n=3)

Table 8- *M.tuberculosis* numbers in lungs and spleen of albino mice - drug and formulation treatment for 18 days

Treatment batch	Log_{10}CFU±SD	
	Lungs	Spleen
Control groups	5.02 ± 0.23	2.16 ± 0.12
Negative control	6.24± 0.32	2.10 ± 0.12
Positive control with INH 25 mg/kg	6.44 ± 0.22	2.10 ± 0.12
Test group with INH-NP's Equivalent to 25 mg/kg	6.28 ± 0.10	2.12 ± 0.10

The data represents mean±SD (n=3)

Table 9- *M.tuberculosis* numbers in lungs and spleen of albino mice - drug and formulation treatment for 6 weeks

Treatment batch	Log_{10}CFU±SD	
	Lungs	Spleen
Control groups	9.82 ± 0.42	4.22 ± 0.14
Negative control	12.2± 0.54	5.64 ± 0.23
Positive control with INH 25 mg/kg	10.24 ± 0.30	3.55 ± 0.24
Test group with INH-NP's Equivalent to 25mg/kg	10.68 ± 0.22	3.14 ± 0.24

The data represents mean±SD (n=3)

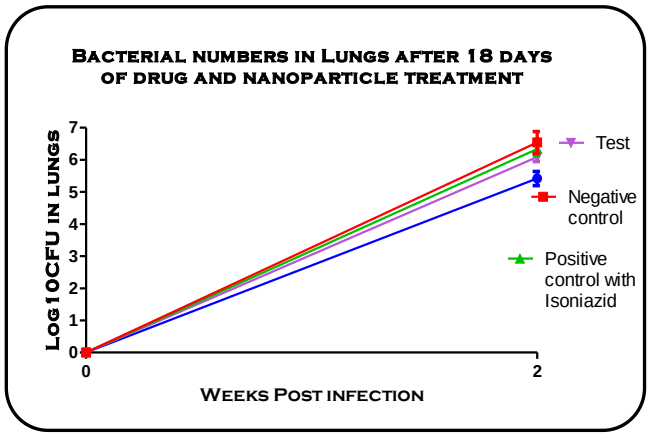

Fig. 12 Determination of bacterial numbers in lungs after 18 days of treatment

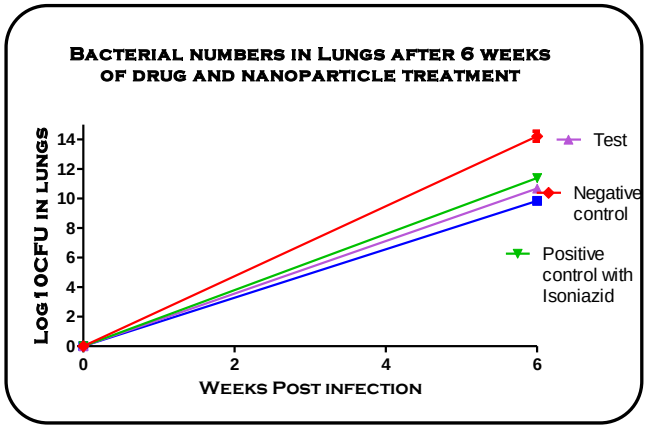

Fig. 13 Determination of bacterial numbers in lungs after 6 weeks of treatment

Determination of morphology by SEM: The samples of F4 freeze dried powder were visualized under SEM photomicrography at 5000X magnification for its structural and morphological characters. The samples were showing characteristic spherical shape and multilamellar smooth arrangement on the particle surface. Moreover, the mean particle diameter was comparable to the data obtained from Zetasizer thus confirming the particle size Figure-3. The spherical shape of the particles might PLGA as reported by Suvimol S., 2015 to enhance mucoadhesion and cell internalizationof carbopol (52)and Dawei D., 2018 for Mucoadhesive PLGA Microparticles for Ocular Drug Delivery (53), Min-HP., 2014 for BSA-loaded eudragit nano particles (54).

FTIR studies: The presence of any possible chemical interaction between INH and PLGA was elucidated by the absorption peaks obtained from FTIR studies. A distinct peaks of INH was observed at 3111.88cm^{-1} (N-H Stretch), 1664.08$cm^{-}1$ (C=O Stretching), 1556.83cm^{-1} (C=N Stretching), 1414.85 cm^{-1} (C=C Stretching), 444.20 cm^{-1} (Aromatic Deformation). Similarly the IR spectra of INH-PLGA mixture portrayed C=O stretch at 1436.22.Bullo S et al., 2016 reported the presence of carbonyl C=O; amino group NH_2; and N–N single bond, C=C double bonds, and a C–H bond of the aromatic ring (55). The INH encapsulated in the PLGA matrix system was found to display characteristic peaks of the drug. The overall infrared spectral results rules out potential interaction between drug (INH) and encapsulating agent (PLGA) and also insists that there is no interference of PLGA for the drug release from the INH-NP's. PLGA with first line anti-tubercular drugs also not showed interference in functional groups presence in first line anti-tubercular drugs as reported by Ruchi C., 2014 (56).

DSC studies: The endothermic peaks of PLGA and INH were found to elute at 62^{o}C (Fig 3a) and 244.2^{o}C (Fig 3b) with their corresponding enthalpies of 149.5J/g and 125.3J/g respectively. In the similar manner the melting temperatures of physical mixtures (PLGA+INH) at 241.4^{o}C (Fig 3c) resulting in enthalpy of 145.2J/g. The endothermic events of INH-NP formulation clearly indicated that the PLGA not affecting significantly and the thermal stability of INH.

Mucoadhesion study

Cytotoxicity Study: In the present study, the cytotoxicity of INH-NP's was tested against A549 (Human lung adenocarcinoma epithelial cells) tumor cells by MTT cytotoxicity method. The INH-NP's was found to be non cytotoxic against A549 cell lines and the IC_{50} value range from 9.6 to 10. The results were present in Table 4 and Figure 4. The mean biodistribution pharmacokinetic parameters of F4 INH-NP formulation administered through IV and Inhalation are summarized in the table 5 and 6, Figure 6 and 7**.** The C_{max}, T_{max} and Clearance of F4 formulation through Inhalation and IV was38.42 ± 4.0 µg/mL, 22 hr, 1.2 and 19.16 ± 3.4 µg/mL, 2 hr, 3.24 respectively. By comparing the Cmax results between IV and Inhalation administration of INH-NP's it shows that greater concentration of drug gets accumulated when administered by inhalational route. From the Tmax comparison data between IV and Inhalation administration it shows the sustainability time of INH-NP's in lungs-confirming the sustained action of F4 formulation in lungs. By comparing the $AUC_{0-\alpha}$ form above tables, it can be concluded that maximum concentration of drug was present in lungs through inhalation than any other organ and the organ clearance ratio of drug from lungs through inhalation was less than the IV administration confirming the sustained release of INH from PLGA Nanospheres in the lungs. Pharmacokinetic distribution data it shows that INH-NP's shows more accumulation of drug in lungs through inhalation administration than IV, which indicates PLGA Nanospheres is being effectively targeted and subsequent sustained release of drug in the lungs. These results confirmed that inhalable PLGA Nanospheres are suitable for targeting with negligible toxicity, maintaining maximum concentration of lung when inhaled, providing sustained release of INH in lungs and improving quality of chemotherapy of pulmonary TB.

***In vivo* and *in vitro* Mycobacterium screening studies:** When INH-NP's was tested against a broad panel of multidrug resistant

clinical isolates like *M. tuberculosis*, it was found to be highly active against all isolates (MIC < 1 g/ml). The activity of INH-NP's against *M. tuberculosis* was also assessed when cultured under conditions of oxygen depletion. INH-NP's demonstrated significant activity when compared to pure drug. In a short-course mouse infection model, the efficacy of INH-NP's at 25 mg/kg of body weight after nine oral treatments was compared with those of INH pure drug. INH-NP's, dose equivalent to 25 mg/kg was more active than pure drug INH at 25 mg/kg. Long-term treatment with INH-NP's at 25 mg/kg reduced the bacterial load most effectively in the lungs and spleen. No significant differences in activity between INH-NP's and the other single drug treatments tested could be observed. The results show that all drug treatments reduced the numbers of CFU in the lungs and spleens significantly at every time point compared with the numbers in the untreated controls (P> 0.001) are depicted in Table 7. After 18 days of treatment, INH-NP's reduced the bacterial loads in the lungs by 0.46 log10 CFU (6.54 versus 6.08 log10 CFU for the untreated controls). The activity of I INH-NP's in the lungs and spleen was statistically not that much different from those of isoniazid pure drug (P < 0.05) after 18 days of treatment. The results are shown in Table 8 and fig. 12. After 6 weeks of treatment, INH-NP's reduced the bacterial loads in the lungs by 3.54 log10 CFU (10.68 versus 14.62 log10 CFU for the untreated controls). The activity of INH-NP's in the lungs and spleen was statistically significant from those of INH pure drug (P > 0.05) after 6 weeks of treatment. The results are depicted in Table 9 and fig. 13. Further, It was shown that on long term therapy INH-NP's resulted in better control of growth of microorganism i.e. colony forming unit (CFU) when compared to short term therapy i.e. for 18 days after inhibition. After 6 weeks of treatment, the bacterial counts in the lungs were reduced to very low numbers in all treatment groups (range, 14.62 to 10.08 log10 CFU of INH-NP's Vs untreated controls), so also in the spleen. There is no complete eradication of the bacterial count in any of the mice after 12 weeks of treatment with single compound as well as the formulation. No statistically significant differences in activity between INH-NP's and the pure drug treatments could be observed for the spleens or the lungs (P > 0.05). In summary, results of evaluation *in vivo* models, as well, against multidrug-resistant M. tuberculosis and against *M. tuberculosis* isolates in a potentially latent state, makes INH-NP's an attractive drug dosage form for the therapy of tuberculosis. These data indicate that there is significant potential for effective delivery of INH-NP's for the treatment of tuberculosis. From the results of *in vivo* screening of *M.tuberculosis*, its effectiveness across *in vivo* models, as well as its activity against multidrug-resistant *M. tuberculosis* and against *M. tuberculosis* isolates in a potentially latent state, makes INH-NP's an attractive drug dosage form for the therapy of pulmonary tuberculosis. These data indicate that there is significant potential anospheres for the treatment of tuberculosis.

CONCLUSION

INH is considered to be the promising and routinely administered antimicrobial agent in treating TB. However, cytotoxic effects and enzymatic degradation by liver are commonly associated limitations with commercially available INH preparations on long term usage. In recent years nanospheres are considered as novel tool for targeted drug delivery systems that is capable of avoiding these toxicological and hepatic first pass effects. A review suggests that drugs having amine (NH_2) group can interact with the polymer dependent group strongly that helps to fasten the rate of polymeric degradation that inturn aids for drug diffusion in the affected site (PLGA Nanoparticles in Drug Delivery: The State of the Art). High pressure homogenization is one of the most efficient encapsulation technique that generates particles of nanomeric range with proven reproducibility. Furthermore, In order to address the stability of prepared nanospheres and to preserve its physicochemical properties, freeze drying in presence of 5% mannitol (cryoprotectant) was found beneficial. Thus formed nanospheres were thought of capable in binding to the tubercular affected cells and show its pharmacological action. The physicochemical characterization such as SEM, DSC and stability studies confirmed the intactness of the

drug inside the PLGA core. The *in vitro* studies and mucoadhesion studies were found to give constructive results for further experimentation *in vivo* using male Wistar rats. The formulated mucoadhesive INH-NP's were capable of binding to the tubercular affected pulmonary site after inhalation in dry form and show better therapeutic efficacy with minimum side effects and its Antitubercular activity of optimized formulation confirmed by its anticancer activity against the human lung adenocarcinoma epithelial cell lines and antimicrobial activity was by inhibiting the growth of Mycobacterium in lung and spleen of mice even after 6 months as it indicating that the lesser drug resistance of Mucoadhesive nanospheres.

REFERENCES

1. Smith JP (2011). Nanoparticle delivery of anti-tuberculosis chemotherapy as a potential mediator against drug-resistant tuberculosis. Yale J Biol Med.84:361-9.
2. Glaziou P, Floyd K Raviglione MC. (2018). Global Epidemiology of Tuberculosis. Semin Respir Crit Care Med. 39:271-285.
3. World Health Organization (WHO), Global tuberculosis report 2018.
4. Lougheed KE, Taylor DL, Osborne SA, Bryans JS, Buxton RS (2009). New anti-tuberculosis agents amongst known drugs. Tuberculosis. 89:364-70.
5. Blomberg B, Spinaci S, Fourie B, Laing R (2001). The rationale for recommending fixed-dose combination tablets for treatment of tuberculosis. Bull World Health Organ.79:61-8.
6. Cohn DL., Bustre F, and Raviglione MC. (1997). Drug-resistant tuberculosis: review of the worldwide situation and the WHO/IUATLD Global Surveillance Project. International Union Against Tuberculosis and Lung Disease. Clin. Infect. Dis. 24:121-130
7. Espinal MA. (2003). The global situation of MDR-TB. Tuberculosis, 83:44-51
8. Zhang Y. (2004). Isoniazid, *In* W. N. Rom and S. M. Garay (ed.), *Tuberculosis*, 2nd ed. Lippincott Williams & Wilkins, New York, NY.739-758.
9. Slayden RA, Barry CE. (2000). The genetics and biochemistry of isoniazid resistance in mycobacterium tuberculosis. Microbes Infect. 2:659-69
10. Quantrill SJ, Woodhead MA, Bell CE, Hardy CC, Hutchison AJ, Gokal R (2002). Side-effects of anti tuberculosis drug treatment in patients with chronic renal failure. Eur Respir J.20:440-3.
11. Patton JS, Byron PR (2007). Inhalingmedicines: deliveringdrugs to the body through the lungs. Nat Rev Drug Discov.6:67-74.
12. Wipaporn R, Narumon C, Ekawat T, Sirirat P, Hak-Kim C and Teerapol S (2011). Isoniazid Proliposome Powders for Inhalation—Preparation, Characterization and Cell Culture Studies. Int J Mol Sci.12: 4414–4434.
13. Kundawala AJ, Patel VA, Patel H V, Choudhary D (2011). Isoniazid loaded chitosan microspheres for pulmonary delivery: Preparation and characterization. Pelagia Res Libr.2:88–97
14. Ahmad Z, Sharma S, Khuller GK (2005). Inhalablealginatenanoparticles as anti tuberculardrugcarriersagainstexperimentalt uberculosis. Int J Antimicrob Agents.26:298-303.
15. Gelperina S, Kisich K, Iseman MD, Heifets L (2005). The potential advantages of nanoparticle drug delivery systems in chemotherapy of tuberculosis. Am J Respir Crit Care Med. 172:1487-90.
16. Sharma D, Sharma RK, Sharma N, Gabrani R, Sharma SK, Ali J, Dang S (2015). Nose-to-Brain delivery of PLGA-Diazepam nanoparticles. AAPS Pharm Sci Tech. 16:1108-21.
17. Seju U, Kumar A, Sawant KK (2011). Development and evaluation of olanzapine-loaded PLGA nanoparticles for nose-to-brain delivery: *in vitro* and *in vivo* studies. Acta Biomater.7:4169-76.
18. Eyles JE, Bramwell VW, Singh J, Williamson ED, Alpar HO (2003). Stimulation of spleen cells *in vitro* by nanospheric particles containing antigen. J Control Release. 86:25–32.
19. Jinwal UK, Groshev A, Zhang J, Grover A, Sutariya VB (2014). Preparation and characterization of methylene blue nanoparticles for Alzheimer's disease and

other tauopathies. Curr Drug Deliv.11:541-50.
20. Li Y, Jiang HL, Zhu KJ, Liu JH, Hao YL (2005). Preparation, characterization and nasal delivery of α-cobrotoxin-loaded poly (lactide-co-glycolide)/ polyanhydride microspheres. J Control Release. 108:10-20.
21. Takeuchi H, Yamamoto H, Kawashima Y (2001). Mucoadhesive nanoparticulate systems for peptide drug delivery. Adv Drug Del Rev. 47:39-54.
22. Bailey BA, Desai KH, Ochyl LJ, Ciotti SM, Moon JJ, Schwendeman SP (2017). Self-encapsulating poly (lactic-co-glycolic acid) (PLGA) microspheres for intranasal vaccine delivery. Mol Pharm.14:3228-37.
23. Arunkumar S, Shivakumar HN, Murthy N (2017). Effect of terpenes on transdermal iontophoretic delivery of diclofenac potassium under constant voltage. Pharm Dev Technol.:1-9.
24. Novak SD, Sporar E, Baumgartner S, Vrecer F (2012). Characterization of physicochemical properties of hydroxypropyl methylcellulose (HPMC) type 2208 and their influence on prolonged drug release from matrix tablets. J Pharm Biomed Anal.136-43.
25. Freire FD, Camara MB, Dantas MG, Aragao CFS, MouraTFADL, Raffin FN (2014). Gastric-resistant Isoniazid pellets reduced degradation of rifampicin in acidic medium. Braz J pharm sci. 50:749-56.
26. Sharma D, Maheshwari D, Philip G, Rana R, Bhatia S, Singh M, Gabrani R, Sharma SK, Ali J, Sharma RK, Dang S (2014). Formulation and optimization of polymeric nanoparticles for intranasal delivery of lorazepam using Box-Behnken design:*In vitro*and*in vivo*evaluation. Biomed Res Int.1-15.
27. Murakami H, Kawashima Y, Niwa T, Hino T, Takeuchi H, Kobayashi M (1997). Influence of the degrees of hydrolyzation and polymerization of poly(vinylalcohol) on the preparation and properties of poly(DL-lactide-*co*-glycolide) nanoparticle. Int J Pharm. 149:43–49.
28. Lee WK, Park JY, Yang EH, Suh H, Kim SH, Chung DS, Choi K, Yang CW, Park JS (2002). Investigation of the factors influencing the release rates of cyclosporin A-loaded micro- and nanoparticles prepared by high-pressure homogenizer. J Control Release. 84:115-23.
29. Silva AC, González-Mira E, García ML, Egea MA, Fonseca J, Silva R, Santos D, Souto EB, Ferreira D (2011). Preparation, characterization and biocompatibility studies on risperidone-loaded solid lipid nanoparticles (SLN): High pressure homogenization versus ultrasound. Colloids Surf B Biointerfaces. 86:158-65.
30. Alihosseini**F**, Ghaffari S, Dabirsiaghi**AR,** Haghighat S (2015). Freeze drying of ampicillin solid lipid nanoparticles using mannitol as cryoprotectant. Braz J pharm sci. 51:797-802.
31. Kocbek P, Obermajer N, Cegnar M, Kos J, Kristl J (2007). Targeting cancer cells using PLGA nanoparticles surface modified with monoclonal antibody. J Control Release.120:18-26.
32. Sondi I, Salopek-Sondi B (2004). Silver nanoparticles as antimicrobial agent: a case study on *E. coli* as a model for Gram-negative bacteria. J Colloid Interface Sci. 275:177-82.
33. Basalus MW, Ankone MJ, Van Houwelingen GK, De Man FH, Von Birgelen C (2009). Coating irregularities of durable polymer based drug eluting stents assessed by scanning electron microscopy. EuroIntervention. 5:157-65.
34. Vaddi HK, Ho PC, Chan SY. (2002). Terpenes in propylene glycol as skin penetration enhancers: permeation and partition of haloperidol, Fourier transform infrared spectroscopy and differential scanning calorimetry. J Pharm Sci. 91:1639-51.
35. Aigner RZ, Sipos EH, Farkas G, Ciurba A, Berkesi O, Szabo-Revesz P (2011).Compatibility studies of aceclofenac with retard tablet excipients by means of thermal and FT-IR spectroscopic methods. J Therm Anal Calorim. 104:265–271.
36. Papadimitriou S,Bikiaris D, Avgoustakis K,Georgarakis M (2008). Chitosan nanoparticles loaded with dorzolamide and pramipexole. Carbohydrate poly. 73:44-54.
37. El-Hameed, MDA, Kellaway IW. (1997). Preparation and *in vitro* characterization of

mucoadhesive polymeric microspheres as intra-nasal delivery systems. Eur J Pharm Biopharm. 44:53-60.
38. Arunkumar S, Shivakumar HN, Desai BG, Ashok P (2016). Effect of gel properties on transdermal iontophoretic delivery of diclofenac sodium, e-Polymers. 16: 25-32.
39. Arunkumar S, Shivakumar HN, Desai BG, Ashok P (2015). Effect of chemical penetration enhancer on transdermal iontophoretic delivery of diclofenac sodium under constant voltage. J Drug Deliv Sci Technol. 30:171-79.
40. Jagtap P, Jadhav K, Dand N (2015). Formulation and *ex vivo* evaluation of solid lipid nanoparticles (SLNS) based hydrogel for intranasal drug delivery. Int J Bioeng Life Sci. 9:43-53.
41. Gavini E, Hegge AB, Rassu G, Sanna V, Testa C, Pirisino G, Karlsen J, Giunchedi P (2006). Nasal administration of carbamazepine using chitosan microspheres: *in vitro/ in vivo* studies. Int J Pharm. 307:9-15.
42. Luppi B, Bigucci F, Corace G, Delucca A, Cerchiara T, Sorrenti M, Catenacci L, Di Pietra AM, Zecchi V (2011). Albumin nanoparticles carrying cyclodextrins for nasal delivery of the anti-Alzheimer drug tacrine. Eur J Pharm Sci.44(4):559-65.
43. Ramaiah B, Nagaraja SH, Kapanigowda UG, Boggarapu PR (2016). Improved Lung concentration of Levofloxacin by targeted gelatin microspheres: *In vivo* pharmacokinetic evaluation of intake rate, targeting efficacy parameters and peak concentration ratio in albino Mice. J Pharm Innov.:1-13.
44. Kapanigowda UG, Nagaraja SH, Ramaiah B, Boggarapu PR, Subramanian R (2015). Enhanced Trans-corneal permeability of valacyclovir by polymethacrylic Acid copolymers based ocular microspheres: *in vivo* evaluation of estimated pharmacokinetic/pharmacodynamic indices and simulation of aqueous humor drug concentration-time profile. J Pharm Innov. 1-12.
45. Jain SK, Jain A, Gupta Y, Kharya A (2008). Design and development of a mucoadhesive buccal film bearing progesterone. Pharmazie, 63:129-135
46. Donald CA Jeremy AH, Quan Y, Andrew Y, Gary LB, and Hu Y (2013). Semi-Interpenetrating Network (sIPN) Gelatin Nanofiber Scaffolds for Oral Mucosal Drug Delivery. Acta Biomater. 9: 6576–6584.
47. Hirenkumar KM and Steven JS (2011), Poly Lactic-*co*-Glycolic Acid (PLGA) as Biodegradable Controlled Drug Delivery Carrier,Polymers (Basel). 3(3): 1377–1397.
48. Rui C, Liu X, Qin F, Man L, Jingjing W, Li W (2017).Hierarchical pulmonary target nanoparticles *via*inhaled administration for anticancer drug delivery. J drug delivery. 24: 1191-1203
49. Gina SE, Gamal MZ (2019). PLGA Nanoparticles Loaded Mucoadhesive and Thermosensitive Hydrogel as a Potential Platform for the Treatment of Oral Mucositis.Int J App Pharm, 11:106-112.
50. Bhosale UV, Devi V K, and Jain N.(2011).Formulation and Optimization of Mucoadhesive Nanodrug Delivery System of Acyclovir. J Young Pharm. 3: 275–283.
51. Pandey J and Tripathi PK. (2016) Formulation and Evaluation of Levocetirizine Loaded Mucoadhesive Microspheres for Nasal Delivery. Int J Pharm Sci Res, 2242-51
52. Suvimol S, Nattika S, Uracha R, Satit P (2015). Surface modification of PLGA nanoparticles by carbopol to enhance mucoadhesion and cell internalization. Colloids and surfaces B: Biointerfaces, 130
53. Dawei D, Binu K, Ambika S, Sindhu V, Saif AK, and Patrick SD (2018). Design of Mucoadhesive PLGA Microparticles for Ocular Drug Delivery. ACS Appl. Bio Mater., 1:561–571
54. Min-HP, Jong SB, Cho AL, Cheong WC (2014). The effect of Eudragit type on BSA-loaded PLGA nanoparticles. Journal of Pharmaceutical Investigation, 44:339-349
55. Bullo S, Mohamed EEZ, Palanisamy A, Sharida F, Thomas JW (2016). Synthesis, characterization, and efficacy of antituberculosis isoniazid zinc aluminum-layered double hydroxide based nanocomposites. Int J Nanomedicine. 11: 3225–3237.
56. Ruchi C, Harshendra SS, Subhash CK, Brahmeshwar M. (2014). Polylactide-co-

glycolide nanoparticles of antitubercular drugs: Formulation, characterization and biodistribution studies, Therapeutic delivery,5:1247-59

57. Zhang N, Chittapuso C, Ampassavate C,Siahaan TJ,and Berkland C (2008). PLGA Nanoparticle-Peptide Conjugate Effectively Targets Intercellular Cell-Adhesion Molecule.Bioconjug Chem. 19: 145–152.
58. Dilip P, Amit KG, Sharad M, Neeraj M, Bhuvaneshwar V, Shailja T, Arvind KJ,and Suresh PV (2010). Evaluation of Mucoadhesive PLGA Microparticles for Nasal Immunization. AAPS J. 2: 130–137.
59. Sinjan D and Dennis HR (2004). Particle size and temperature effect on the physical stability of PLGA nanospheres and microspheres containing BodipyAAPS PharmSciTech. 5: 18–24.
60. Long-Bin C, Sha Z, and Wei Z (2016). Highly Stable PEGylated Poly(lactic-co-glycolic acid) (PLGA) Nanoparticles for the Effective Delivery of Docetaxel in Prostate Cancers.Nanoscale Res Lett.; 11: 305.